International Journal of Modern Physics D
Vol. 16, Nos. 2&3 (2007) 411–420

World Scientific
www.worldscientific.com

A NOTE ON THE LARGE-ANGLE ANISOTROPIES IN THE WMAP CUT-SKY MAPS

A. BERNUI

Instituto Nacional de Pesquisas Espaciais – Divisão de Astrofísica,
Av. dos Astronautas 1758,
12227-010 São José dos Campos – SP, Brazil

B. MOTA and M. J. REBOUÇAS

Centro Brasileiro de Pesquisas Físicas,
Rua Dr. Xavier Sigaud 150, 22290-180 Rio de Janeiro – RJ, Brazil

R. TAVAKOL

Astronomy Unit – School of Mathematical Sciences, Queen Mary,
University of London, Mile End Road, London E1 4NS, UK

Received 21 December 2005
Communicated by B. E. J. Bodmann

Recent analyses of the WMAP data seem to indicate the possible presence of large-angle anisotropy in the Universe. If confirmed, these can have important consequences for our understanding of the Universe. A number of attempts have recently been made to establish the reality and nature of such anisotropies in the CMB data. Among these is a directional indicator recently proposed by the authors. A distinctive feature of this indicator is that it can be used to generate a sky map of the large-scale anisotropies of the CMB maps. Applying this indicator to full-sky temperature maps we found a statistically significant preferred direction. The full-sky maps used in these analyses are known to have residual foreground contamination as well as complicated noise properties. Thus, here we performed the same analysis for a map where regions with high foreground contamination were removed. We find that the main feature of the full-sky analysis, namely the presence of a significant axis of asymmetry, is robust with respect to this masking procedure. Other subtler anomalies of the full-sky are on the other hand no longer present.

Keywords: Observational cosmology; cosmic microwave background; large-scale anisotropies in CMB; large-angle anomalies in CMB.

1. Introduction

The wealth of high resolution data provided by the Wilkinson Microwave Anisotropy Probe (WMAP)[1,2] has confirmed to very good approximation the standard cosmological picture, which predicts a statistically isotropic Gaussian random cosmic microwave background (CMB) temperature fluctuations. Despite this success, several large-scale anomalies in the CMB have been reported including

indications of non-Gaussianity,[3−12] evidences for a North-South asymmetry,[13] and the so-called "low-ℓ anomalies" such as the surprisingly small values of the CMB quadrupole and octopole moments,[15] and the alignment of the quadrupole and octopole moments,[16−18] (in this connection see Ref. 19) whose direction has been suggested to extend to the higher multipoles[20] (see also Ref. 21 for a detailed discussion). In addition, there are also indications for a preferred axis of symmetry or directions of maximum asymmetry.[22−29]

The possible origins of such unexpected anomalous features of CMB are at present the object of intense investigation, with several potential explanations, including unsubtracted foreground contamination and/or systematics,[27] unconsidered local effects,[30,31] other mechanisms to break statistical isotropy,[32,33] and also extra-galactic origin (see Refs. 13, 16, 20 and 22–26 for details). If they turn out to have a cosmological nature, however, they could have far reaching consequences for our understanding of the Universe, in particular for the above-mentioned standard cosmological scenario.

Recently we proposed[34] a new directional indicator $\sigma = \sigma(\theta, \phi)$, based on pair angular separation histogram (PASH),[35] to measure large-angle anisotropy in the WMAP data. An important feature of our indicator is that it can be used to generate a sky map of large-angles anisotropies from CMB temperature fluctuations maps. We have produced and studied in details σ-maps generated from the full-sky LILC,[38] "cleaned" TOH,[16] and co-added[2] WMAP maps, and found a statistically significant preferred direction in these WMAP maps, which agrees with the preferred asymmetry axes recently reported.[13,26] These results were found to be robust with respect to the choice of the full-sky WMAP CMB maps employed. However, since full-sky maps are known to have residual foreground contamination[38] and complicated noise properties,[2] their choice in the "low-ℓ" studies is not a consensus.[21,39] Thus, the question arises as to whether our results hold for cut-sky maps. Our main aim here, which extends and complements our previous work,[34] is to address this question by considering the LILC map with a Kp2 sky cut. To this end, in the next section we give an account of our large-angle anisotropy indicator, while in the last section we apply our indicator to the LILC map with a Kp2 sky cut, and present our main results and conclusions.

2. Large-Angle Anisotropy Indicator

For a detailed discussion of the indicator briefly presented in this section we refer the readers to Ref. 34.

The key point in the construction of our indicator is that a homogeneous distribution of points on a two-sphere S^2 is seen by an observer at the center of S^2 as isotropically distributed, and therefore deviations from homogeneity in this distribution give rise to anisotropies for this observer.

Mutatis mutandis, since in CMB studies the celestial sphere is discretized into a set of equal size pixels, with a temperature fluctuation associated to each pixel, the

idea in the CMB context is then to construct an indicator that measures deviation from homogeneity in the distribution of pixels with similar temperature. The first step towards the construction of this indicator is subdivide a given CMB map into a number of submaps, each consisting of equal number of pixels with similar temperatures. The next step is to devise an indicator to measure the deviation from a homogeneous distribution of these pixels. The construction of our indicator, $\sigma = \sigma(\theta, \phi)$ is based on angular separation histograms (PASH), which are obtained by counting the number of pairs of pixels whose angular separation α lies within small sub-intervals (bins) $J_i \in (0, \pi]$, of length $\delta\alpha = \pi/N_{\rm bins}$, where

$$J_i = \left(\alpha_i - \frac{\delta\alpha}{2},\ \alpha_i + \frac{\delta\alpha}{2}\right], \quad i = 1, 2, \ldots, N_{\rm bins},$$

with the bin centers at $\alpha_i = (i - \frac{1}{2})\,\delta\alpha$. The PASH is then defined as the following normalized function

$$\Phi(\alpha_i) = \frac{2}{n(n-1)}\frac{1}{\delta\alpha}\sum_{\alpha\in J_i}\eta(\alpha), \tag{1}$$

where n is the total number of pixels in the submap, $\eta(\alpha)$ is the number of pairs of pixels with separation $\alpha \in J_i$, and where the normalization condition $\sum_{i=1}^{N_{\rm bins}} \Phi(\alpha_i)\delta\alpha = 1$ holds.

Now, for a distribution of n pixels in the sky sphere S^2 one can compute the expected number of pairs, $\eta_{\rm exp}(\alpha)$ with angular separation $\alpha \in J_i$. From this quantity one obtains the normalized expected pair angular separation histogram (EPASH), which is clearly given by

$$\Phi_{\rm exp}(\alpha_i) = \frac{1}{N}\frac{1}{\delta\alpha}\sum_{\alpha\in J_i}\eta_{\rm exp}(\alpha) = \frac{1}{\delta\alpha}P(\alpha_i) = \mathcal{P}(\alpha_i), \tag{2}$$

where $N = n(n-1)/2$ is the total number of pairs of pixels, $P(\alpha_i) = \sum_{\alpha\in J_i}\eta_{\rm exp}(\alpha)/N$ is the probability that a pair of objects can be separated by an angular distance that lies in the interval J_i, $\mathcal{P}(\alpha_i)$ is the corresponding probability density, and where the coefficient of the summation is a normalization factor. Equation (2) makes it clear that the EPASH $\Phi_{\rm exp}(\alpha)$ gives the distribution of probability of finding pairs of points on the sky sphere with any angular separation $\alpha_i \in (0, \pi]$.[a] We denote the difference between the mean PASH (MPASH),

[a]For a homogeneous and continuous distribution of points on S^2 all angular separations $0 < \alpha \leq \pi$ are allowed, and the corresponding probability distribution can be calculated to give[35] $\Phi_{\rm exp}(\alpha) = \mathcal{P}(\alpha) = \frac{1}{2}\sin\alpha$. This is the limit of a statistically isotropic distribution of points in S^2 as the number of points go to infinity. One can thus quantify anisotropy by calculating the departure of the mean observed probability distribution $\langle\Phi_{\rm obs}(\alpha_i)\rangle$ from it, namely $\langle\Phi_{\rm obs}(\alpha_i)\rangle - \Phi_{\rm exp}(\alpha_i)$.

$\langle\, \Phi_{\rm obs}(\alpha_i)\,\rangle$, calculated from the observational data, and the EPASH $\langle\Phi_{\rm exp}(\alpha_i)\rangle$, obtained from an statistically isotropic distribution of pixels, as

$$\Upsilon(\alpha_i) \equiv \langle\Phi_{\rm obs}(\alpha_i)\rangle - \Phi_{\rm exp}(\alpha_i). \tag{3}$$

In practice, the expected $\Phi_{\rm exp}(\alpha_i)$ for a statistically isotropic map is obtained simply by scrambling a CMB map multiple times, and averaging over the resulting histograms.

Lastly, to quantify anisotropy, we distill the histogram $\Upsilon(\alpha_i)$ into a single number, by defining the indicator $\sigma = \sigma(\theta,\phi)$ as the variance of $\Upsilon(\alpha_i)$ (which has zero mean), namely

$$\sigma^2(\theta,\phi) \equiv \frac{1}{N_{\rm bins}} \sum_{i=1}^{N_{\rm bins}} \Upsilon^2(\alpha_i). \tag{4}$$

Calculating σ for the whole celestial sphere would yield a global measure of anisotropy. To obtain a directional indicator, we can instead calculate both MPASH and EPASH for spherical-shaped caps. The indicator σ can then be viewed as a (nonlocal) measure of the anisotropy in the direction of the center of the cap. Thus, by construction, $\sigma(\theta,\phi)$ measures the deviation from isotropy in a given direction, i.e. how the observed distribution of points deviates from a statistically isotropic one.[b]

Since σ is a discrete scalar function defined on S^2, it can be expanded in spherical harmonics, and its power spectrum D_ℓ can be calculated, namely

$$\sigma(\theta,\phi) = \sum_{\ell=0}^{\infty} \sum_{m=-\ell}^{\ell} b_{\ell m}\, Y_{\ell m}(\theta,\phi) \quad \text{and} \quad D_\ell = \frac{1}{2\ell+1} \sum_m |b_{\ell m}|^2. \tag{5}$$

It then follows that if a large-angle asymmetry is present in the CMB temperature distribution, it should significantly affect the σ-map on the corresponding angular scales (low-ℓ multipoles).

In the next section, we shall generate the σ-maps from LILC map with a Kp2 sky cut, study its main features, and make a comparison with our previous results for the full-sky CMB maps.[34]

3. Main Results and Conclusions

Given that the large-scale angular correlations are nonlocal, $\sigma(\theta,\phi)$, calculated over a 30°-radius cap centered at (θ,ϕ), can be though of as a measure of the anisotropy in the direction (θ,ϕ). In our previous work[34] the strategy was to obtain σ for a set of 12,288 caps of radius 30° co-centered with the same number of pixels generated by HEALPix with $N_{\rm side} = 32$, evenly covering the entire celestial sphere. The resulting directional map of anisotropy was the so-called σ-map. We applied

[b]Incidentally, for a homogeneous and continuous distribution of points on S^2 the EPASH for a cap of aperture $\theta_0 \leq \pi/2$ can also be calculated in a closed form,[37] but in practice one approximates $\Phi^{\rm CAP}_{\rm exp}(\alpha_i)$ by the MPASH $\langle\Phi^{\rm CAP}_{\rm exp}(\alpha_i)\rangle$ of the statistically isotropic distribution of pixels.

this new anisotropy indicator to three CMB WMAP maps: the LILC[38] and the TOH[16] maps (which are two differently foreground cleaned full-sky maps resulting from the combination of the five frequency bands: K, Ka, Q, V, and W CMB maps measured by the WMAP satellite), and the co-added map, which is a weighted combination of the Q, V, and W WMAP maps.

The resulting σ-map were found to be anisotropic. Briefly, there is a prominent spot with very high σ on the southeastern corner, with a well defined maximum at ($b \simeq 115°, l \simeq 235°$), which is close (by 16°) to the direction recently indicated in Ref. 11. It was further shown (by a standard spherical harmonics expansion) that the LILC σ-map deviates from isotropy in a statistically significant way, with anomalously high ($> 95\%$ CL) dipole, quadrupole and octopole components (see Figs. 3 and 4 of Ref. 34). The higher components on the other hand fall within the expected values. This clearly indicates that the LILC map is not statistically isotropic. Finally, we noted that the quadrupole component has a very peculiar shape, being very symmetric around an axis slightly off the galactic North-South. Indeed, 82% of the total power in D_2 comes from an axisymmetric component in the direction ($b = 10°, l = 289°$), somewhat close to the axes of symmetry of the temperature quadrupole and octopole found in Ref. 16 (about 24° from both).

As previously mentioned, however, there is no consensus as to whether the full sky cleaned maps available are indeed free of significant galactic contamination. The question then arises as to whether one should study the full sky maps or confine the analysis to regions where such contamination is small.

In view of the lack of consensus on how to perform the data analysis, here we examine the robustness of our previous results by investigating the LILC map after the application of the Kp2 mask (hereafter the LILC-Kp2 map), which discards the temperature fluctuations of 15.3% of the total number of pixels, mainly concentrated around the galactic plane.

Note that some of the caps with centers close to but outside the Kp2 mask would still overlap with the mask itself. If the intersection region is too large the σ value would be largely an artifact of the masking procedure. On the other hand, if we were to exclude all caps were any overlapping occurs, we would lose information on over half of the sky. To achieve a balance, we shall disregard caps that obey either of the following criteria:

- have the cap center within the Kp2 mask, and
- have over 15% of pixels within the Kp2 mask.

With this critical value of 15% for the maximum number of overlapping pixels typically the value of σ calculated for the same cap in both the LILC and LILC-Kp2 maps differ by less than 10%.

As can be seen in Fig. 1, there is a spot of very high σ in the southeastern corner of the map, which coincides in both direction and magnitude with the one found in

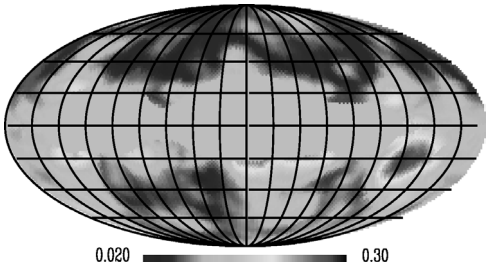

Fig. 1. The σ-map for the LILC-Kp2 map. This result was obtained by calculating σ for spherical caps with aperture $\theta_0 = 30°$, following the criteria outlined above.

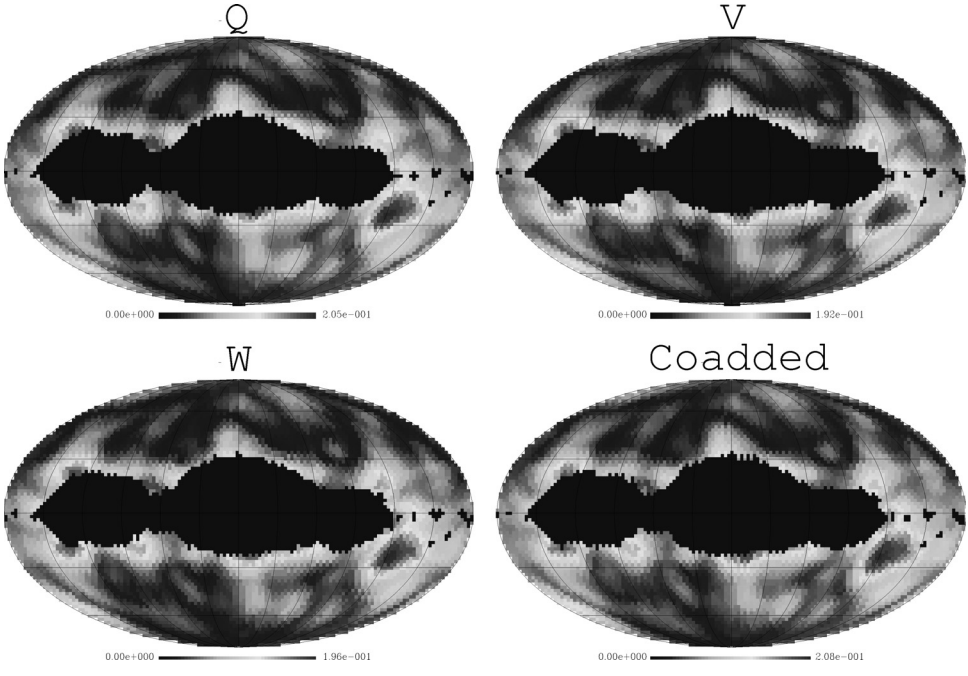

Fig. 2. The σ-map for the WMAP's Q-, V- and W-bands, along with the combined co-added map, using the Kp2 mask. In all maps the high σ value is apparent.

the full LILC σ-map.[34] The fact that this spot lies well outside the region of significant galactic contamination suggests it is not the result of galactic contamination. The possibility remains, however, that it is caused by some unaccounted foreground contamination. Such contamination however would unlikely affect the different frequency bands in exactly the same way. To verify whether this is the case, we calculated the σ-map for the Q-, V- and W-bands separately, along with the co-added map,[40] which is considered the most reliable map for CMB studies[38,39] (see Fig. 2). The resulting maps are almost identical, supporting the result that foreground contamination may not account for the previously reported[34] large scale anisotropy.

Several new smaller high σ spots are also in evidence near the mask region, but they are probably just artifacts of the masking procedure. As discussed in Ref. 34 the main features of the resulting σ-map are robust with respect to the number of spherical caps used to cover the celestial sphere or the cap aperture θ_0.

To obtain more quantitative information about the observed anisotropy, we followed the procedure of our previous work and calculated the power spectrum of the LILC-Kp2 σ-map using the Anafast subroutine in Healpix.[41] Since we are now dealing with an incomplete sphere, the spherical harmonics are no longer orthogonal, and the values obtained must be handled with care. The D_l values are depicted in Fig. 3, along with the corresponding full sky values for comparison. It is clear that the dipole component of the σ-map is even larger for the LILC-Kp2 than for the full sky LILC. This is consistent with the presence of an axis of asymmetry, again confirming our earlier results. The direction of the σ-map dipole changes, however, from $(b = 141°, l = 240°)$ in the full sky map to $(b = 150°, l = 209°)$, in the LILC-Kp2 map, a difference of 19°. The quadrupole and octopole components on the other hand are comparatively smaller in the LILC-Kp2 map, probably due to the fact that many of the high σ structures other than the large spot in the southeastern quadrant are now excluded by the Kp2 mask.

Another feature missing from the LILC-Kp2 σ-map is the peculiar shape of the quadrupole component observed in the full sky map. In the latter case, 82% of the total power in D_2 comes from an axisymmetric component in the direction $(b = 10°, l = 289°)$, which may be related to the observed alignment of the temperature quadrupole and octopole.

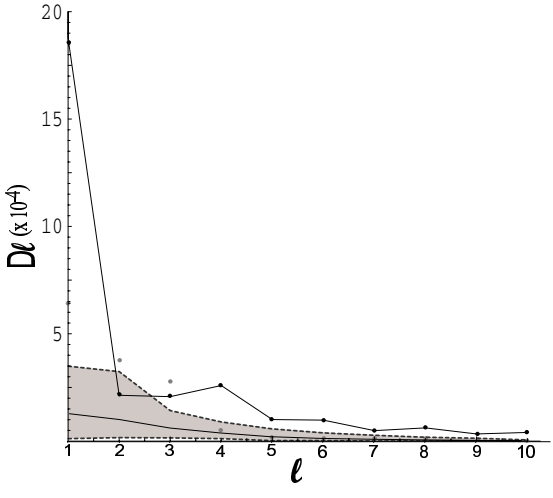

Fig. 3. The power spectrum of the LILC-Kp2 (black dots) and LILC (gray dots) σ-maps for $\ell = 1, \ldots, 10$. For comparison, the average σ-map power spectrum for a set of statistically isotropic full skies is shown (solid curve within the gray band), along with its 95% confidence limits (dashed curves).

We have shown that a large scale anisotropy, roughly resembling an axis of asymmetry, remains a feature of the CMB sky even if the regions where galactic contamination is large are not taken into account. Its essential dipolar nature in particular is a very robust feature, and is consistent with other axes reported in the literature obtained using different methods. This strongly suggests that either the observable universe is intrinsically anisotropic, or that there are other, subtler forms of foreground contamination that have not yet been taken into account. Among the proposed explanations for the global preferred direction, it has been suggested that it could be due to a non-trivial topology of the spatial section of the universe[15,21] (for more details on cosmic topology see the review articles Refs. 42, and, e.g., Refs. 46–66). If topology is indeed the origin, the indicator Υ is promising in distinguishing between different topologies, as has been demonstrated by computer simulations in Ref. 35. These are very exciting possibilities, and are worthy of further investigation.

Acknowledgments

We thank CNPq, PCI-CBPF/CNPq, PCI-INPE/CNPq and PPARC for the grants under which this work was carried out. We acknowledge use of the Legacy Archive for Microwave Background Data Analysis (LAMBDA). Some of the results in this paper have been derived using the HEALPix package.

References

1. C. L. Bennett *et al.*, *Astrophys. J.* **583** (2003) 1.
2. C. L. Bennett *et al.*, *Astrophys. J. Suppl.* **148** (2003) 1.
3. C. J. Copi, D. Huterer and G. D. Starkman, *Phys. Rev. D* **70** (2004) 043515.
4. E. Komatsu *et al.*, *Astrophys. J. Suppl.* **148** (2003) 119.
5. C.-G. Park, *Mon. Not. R. Astron. Soc.* **349** (2004) 313.
6. L.-Y. Chiang, P. D. Naselsky, O. V. Verkhodanov and M. J. Way, *Astrophys. J.* **590** (2003) L65.
7. P. Vielva, E. Martinez-Gonzalez, R. B. Barreiro, J. L. Sanz and L. Cayon, *Astrophys. J.* **609** (2004) 22.
8. H. K. Eriksen, A. J. Banday, K. M. Gorski and P. B. Lilje, *Astrophys. J.* **622** (2005) 58.
9. D. L. Larson and B. D. Wandelt, *Astrophys. J.* **613** (2004) L85.
10. P. Coles, P. Dineen, J. Earl and D. Wright, *Mon. Not. R. Astron. Soc.* **350** (2004) 983.
11. P. D. Naselsky, L.-Y. Chiang, P. Olesen and O. V. Verkhodanov, *Astrophys. J.* **615** (2004) 45.
12. A. Bernui, C. Tsallis and T. Villela, to appear in *Phys. Lett. A* (2006), astro-ph/0512267.
13. H. K. Eriksen, F. K. Hansen, A. J. Banday, K. M. Gorski and P. B. Lilje, *Astrophys. J.* **605** (2004) 14. [Erratum *Astrophys. J.* **609** (2004) 1198].
14. A. Bernui, T. Villela, C. A. Wuensche, R. Leonardi and I. Ferreira, to appear in *Astron. Astrophys.* (2006), astro-ph/0601593.
15. D. N. Spergel *et al.*, *Astrophys. J. Suppl.* **148** (2003) 175.
16. M. Tegmark, A. de Oliveira-Costa and A. J. S. Hamilton, *Phys. Rev. D* **68** (2003) 123523.

17. A. de Oliveira-Costa, M. Tegmark, M. Zaldarriaga and A. Hamilton, *Phys. Rev. D* **69** (2004) 063516.
18. J. R. Weeks, astro-ph/0412231.
19. Y. Wiaux, P. Vielva, E. Martinez-Gonzalez and P. Vandergheynst, astro-ph/0603367.
20. K. Land and J. Magueijo, *Phys. Rev. Lett.* **95** (2005) 071301.
21. C. J. Copi, D. Huterer, D. J. Schwarz and G. D. Starkman, *Mon. Not. R. Astron. Soc.* **367** (2006) 79.
22. E. F. Bunn and D. Scott, *Mon. Not. R. Astron. Soc.* **313** (2000) 331.
23. F. K. Hansen, A. J. Banday and K. M. Gorski, *Mon. Not. R. Astron. Soc.* **354** (2004) 641.
24. F. K. Hansen, P. Cabella, D. Marinucci and N. Vittorio, *Astrophys. J.* **607** (2004) L67.
25. T. Wibig and A. W. Wolfendale, *Mon. Not. R. Astron. Soc.* **360** (2005) 236.
26. K. Land and J. Magueijo, *Mon. Not. R. Astron. Soc.* **357** (2005) 994.
27. D. J. Schwarz, G. D. Starkman, D. Huterer and C. J. Copi, *Phys. Rev. Lett.* **93** (2004) 221301.
28. S. Prunet, J.-P. Uzan, F. Bernardeau and T. Brunier, *Phys. Rev. D* **71** (2005) 083508.
29. E. P. Donoghue and J. F. Donoghue, *Phys. Rev. D* **71** (2005) 043002.
30. C. Vale, astro-ph/0510137.
31. A. Cooray and N. Seto, astro-ph/0509039.
32. C. Gordon, W. Hu, D. Huterer and T. Crawford, astro-ph/0509301.
33. K. Tomita, astro-ph/0509518.
34. A. Bernui, B. Mota, M. J. Rebouças and R. Tavakol, astro-ph/0511666.
35. A. Bernui and T. Villela, astro-ph/0511339.
36. A. Bernui and T. Villela, *Astron. Astrophys.* **445** (2006) 795.
37. A. F. F. Teixeira, physics/0312013.
38. H. K. Eriksen, A. J. Banday, K. M. Gorski and P. B. Lilje, *Astrophys. J.* **612** (2004) 633.
39. P. Bielewicz, H. K. Eriksen, A. J. Banday, K. M. Gorski and P. B. Lilje, astro-ph/0507186.
40. G. Hinshaw *et al.*, *Astrophys. J. Suppl.* **148** (2003) 135.
41. K. M. Górski, E. Hivon, A. J. Banday, B. D. Wandelt, F. K. Hansen, M. Reinecke and M. Bartelman, *Astrophys. J.* **622** (2005) 759.
42. M. Lachièze-Rey and J.-P. Luminet, *Phys. Rep.* **254** (1995) 135.
43. G. D. Starkman, *Class. Quant. Grav.* **15** (1998) 2529.
44. J. Levin, *Phys. Rep.* **365** (2002) 251.
45. M. J. Rebouças and G. I. Gomero, *Braz. J. Phys.* **34** (2004) 1358 [astro-ph/0402324].
46. R. Lehoucq, M. Lachièze-Rey and J.-P. Luminet, *Astron. Astrophys.* **313** (1996) 339.
47. B. F. Roukema and A. Edge, *Mon. Not. R. Astron. Soc.* **292** (1997) 105.
48. N. J. Cornish, D. Spergel and G. Starkman, *Class. Quant. Grav.* **15** (1998) 2657.
49. J. R. Bond, D. Pogosyan and T. Souradeep, *Phys. Rev. D* **62** (2000) 043005.
50. J. R. Bond, D. Pogosyan and T. Souradeep, *Phys. Rev. D* **62** (2000) 043006.
51. G. I. Gomero, A. F. F. Teixeira, M. J. Rebouças and A. Bernui, *Int. J. Mod. Phys. D* **11** (2002) 869.
52. H. V. Fagundes and E. Gausmann, *Phys. Lett. A* **261** (1999) 235.
53. J.-P. Uzan, R. Lehoucq and J.-P. Luminet, *Astron. Astrophys.* **351** (1999) 766.
54. M. J. Rebouças, *Int. J. Mod. Phys. D* **9** (2000) 561.
55. G. I. Gomero, M. J. Rebouças and A. F. F. Teixeira, *Phys. Lett. A* **275** (2000) 355.
56. G. I. Gomero, M. J. Rebouças and A. F. F. Teixeira, *Class. Quant. Grav.* **18** (2001) 1885.

57. B. Mota, G. I. Gomero, M. J. Rebouças and R. Tavakol, *Class. Quant. Grav.* **21** (2004) 3361.
58. J.-P. Luminet, J. Weeks, A. Riazuelo, R. Lehoucq and J.-P. Uzan, *Nature* **425** (2003) 593.
59. R. Aurich, S. Lustig and F. Steiner, *Class. Quant. Grav.* **22** (2005) 2061.
60. R. Aurich, S. Lustig and F. Steiner, *Class. Quant. Grav.* **22** (2005) 3443.
61. W. S. Hipolito-Ricaldi and G. I. Gomero, *Phys. Rev. D* **72** (2005) 103008.
62. G. I. Gomero, M. J. Rebouças and R. Tavakol, *Class. Quant. Grav.* **18** (2001) 4461.
63. G. I. Gomero, M. J. Rebouças and R. Tavakol, *Class. Quant. Grav.* **18** (2001) L145.
64. G. I. Gomero, M. J. Rebouças and R. Tavakol, *Int. J. Mod. Phys. A* **17** (2002) 4261.
65. J. R. Weeks, R. Lehoucq and J.-P. Uzan, *Class. Quant. Grav.* **20** (2003) 1529.
66. J. R. Weeks, *Mod. Phys. Lett. A* **18** (2003) 2099.
67. B. Mota, M. J. Rebouças and R. Tavakol, *Class. Quant. Grav.* **20** (2003) 4837.